ACOUSTICS 2012

Random excitation by optimized pulse inversion in contrast harmonic imaging

S. Ménigot and J.-M. Girault

Imagerie et cerveau, Hôpital Bretonneau 1 Bd Tonnelle 37044 Tours
sebastien.menigot@etu.univ-tours.fr

Over the past twenty years, in ultrasound contrast imaging, new physiological information are obtained by the detection of non-linearities generated by the microbubbles. One of the most used techniques is the pulse inversion imaging. The usual command of this system is a fixed-frequency sinus wave. An optimal choice of this command requires the knowledge of the transducer and of the medium to obtain the best contrast-to-tissue ratio. However, these information are experimentally inaccessible. Our goal is to seek the command which maximizes the contrast-to-tissue ratio. Among several noises, we identified the one which maximized the contrast-to-tissue ratio. A new suboptimal control was made from the parameters of a nonlinear autoregressive filter and from suboptimal noise. The contrast-to-tissue ratio was then iteratively optimized by the method of Nelder-Mead which adjusted the filter parameters. The gain compared to the case in which we used at the optimal frequency can reach about 1 dB and 5 dB in comparison to the center frequency of the transducer. By adding a closed loop, the system automatically proposes the optimal command without any *a priori* knowledge of the system or of the medium explored and without any hypothesis about the shape of the command.

1 Introduction

Over the past twenty years, improvements in sensitivity of medical ultrasound imaging systems have provided more accurate medical diagnoses through intravenous injection of ultrasound contrast agents containing microbubbles. The perfusion imaging thus obtained has provided physiological and pathological information [1]. The use of ultrasound contrast imaging was revolutionized in clinical practice when the nonlinear interaction was taken into account. The nonlinearity of contrast agent responses has become a major focus of research to obtain the best contrast. However, obtaining an ideal method has been limited by two factors. First, good separation of the harmonic components requires a limited pulse bandwidth [2], which reduces the axial resolution as in second harmonic imaging [3], and secondly the effects of the ultrasound wave propagation limit the contrast-to-tissue ratio (*CTR*) because of the presence of nonlinear components generated in tissue [1].

Several imaging methods have been proposed to improve contrast and/or resolution. Some techniques have been only based on post-processings, such as second harmonic imaging [3], subharmonic imaging [4], super harmonic imaging [5] or attenuation correction [6]. Other imaging methods are based on post-processings with encoding which can enable to increase the contrast while ensuring a good axial resolution: the pulse inversion imaging [7], power modulation [8], contrast pulse sequencing [9], pulse subtraction [10] and harmonic chirp imaging [11]. The one of the most commonly used is the pulse inversion imaging, that is reason why this study focused on this technique.

For optimally using the pulse inversion imaging, the transmitted pulse must be correctly chosen. The problem is to find the optimal command $x^\star(t)$ of the pulse inversion imaging system which provides the best *CTR*:

$$x^\star(t) = \arg\max_{x(t)} \left(CTR\left(x(t)\right)\right), \tag{1}$$

Nowadays, any method can solve satisfactorily and optimally this problem [12]. The first solution is an analytic solution developped by Reddy and Szeri [13]. Unfortunately, the problem solution requires (i) inaccessible knowledges *a priori* of the medium and the transducer and (ii) hard solver implementation. The second solution carried on regardless the previous difficulties to transform the shape optimization in a suboptimal parametric optimization; for example the transmit frequency [14]. Nevertheless, these techniques have been shown that it was important to find the optimal command to maximize the *CTR*.

The aim of this study was to find the shape of the optimal command. However, since the problem of the optimal command was difficult to solve directly, we proposed another way to improve the existing optimization method by using randomness and which we applied in simulation. The advantage of the method was the optimization without *a priori* knowledge in order to find the optimal shape.

2 Optimal Command Principle

The principle of the optimal command research for pulse inversion imaging was based on randomness and the Monte-Carlo method (switches on position 1 in Fig 1). For a case k, a random pulse $x_{1,k}(t)$ and the same signal in opposite phase $x_{2,k}(t)$ were transmitted. The sum $z_k(t)$ of the two respective echoes $y_{1,k}(t)$ and $y_{2,k}(t)$ formed a radiofrequency line of the image. This test was repeated many times until find random pulse which maximize the *CTR*.

However, this research was time consuming. After a limited random research, the *CTR* optimization became a parametric optimization using the best previous random excitation (switches on position 2 in Fig 1).

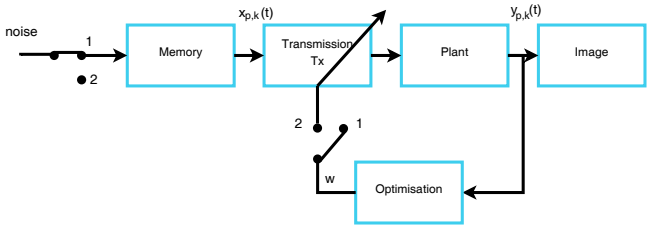

Figure 1: Block diagram of the optimization process. If the switches were on position 1, the optimization was lead by the Monte-Carlo method, and if the switches were on position 2, the optimization was lead by the parametric optimization. The plant included the imaging method, the transducers and the explored medium.

2.1 Random Excitation

The random pulse signal $x_{1,k}(t)$ was computed digitally with Matlab (Mathworks, Natick, MA, USA):

$$x_{1,k}(t) = A \cdot w_{1,k}(t). \tag{2}$$

The white noise modulated by a Gaussian function [11] $w_{1,k}(t)$ was constructed such as:

$$w_{1,k}(t) = \exp\left[-\frac{(t-t_0)^2}{\sigma}\right] n_k(t), \quad (3)$$

where t is the time, t_0 the time for which the Gaussian function is maximum, σ the Gaussian width set so that the signal bandwidth was equals to the transducer bandwidth, and $n_k(t)$ was the k-th white noise computed from normally distributed pseudorandom numbers.

The amplitude of the driving pressure A was then adjusted so that the energy of the pulse $x_{1,k}(t)$ was constant for each case k:

$$A = \sqrt{\frac{A_0^2 \cdot E_{x_{ref}}}{E_w}}, \quad (4)$$

where A_0 is the driving pressure amplitude of the reference signal x_{ref}. This signal x_{ref} was modulated sinus signal at the centre frequency of the transducer. Its energy $E_{x_{ref}}$ constituted the reference energy, while E_w was the energy of the signal $w_{1,k}$. The energy of the transmitted wave thus remained constant by adjusting the amplitude signal A.

The random pulse signal in opposite phase $x_{2,k}(t)$ was then computed such as:

$$x_{2,k}(t) = -x_{1,k}(t). \quad (5)$$

These signals $x_{1,k}(t)$ and $x_{2,k}(t)$ were filtered by the transducer and were then transmitted to the medium.

2.2 Cost-function

In the receiver, CTR_k was computed from a line $z_k(t)$ of pulse inversion image:

$$z_k(t) = y_{1,k}(t) + y_{2,k}(t), \quad (6)$$

where $y_{p,k}(t)$ is the echo of the transmitted pulse $x_{p,k}(t)$ with $p = \{1, 2\}$. It is defined as the ratio of the energy $E_{b,k}$ backscattered by the area of the perfused medium and the energy $E_{t,k}$ backscattered by the area of the non-perfused medium [15] as follows:

$$CTR_k = 10 \cdot \log_{10}\left(\frac{E_{b,k}}{E_{t,k}}\right), \quad (7)$$

These energies were measured from the lines $z_k(t)$ at iteration k of the pulse inversion image.

2.3 Parametric Optimization

Since the random process was time-consuming, we transformed the problem in a parametric optimization. From the best random excitation $x_{1,k^\star}(t)$ obtained previously, the optimization algorithm set the parameters θ of a nonlinear autoregressive filter and the problem became:

$$\theta^\star = \arg\max_\theta \left[CTR\left(\hat{x}\left(t,\theta\right)\right)\right], \quad (8)$$

where $\theta^\star$ were the optimal parameters. The signal $\hat{x}(t,\theta)$ was modelized by the nonlinear autoregressive filter such as:

$$\hat{x}(t) = \mathbf{x}_t^T \theta \quad (9)$$

where ^{T} is the transpose symbol and

$$\begin{aligned}\mathbf{x}_t = [&x_{1,k^\star}(t), x_{1,k^\star}(t-1), \ldots, x_{1,k^\star}(t-M+1),\\ &x^2_{1,k^\star}(t), x_{1,k^\star}(t)x_1(t-1), \ldots, x^2_{1,k^\star}(t-M+1),\\ &x^3_{1,k^\star}(t), x^2_{1,k^\star}(t)x_1(t-1), \ldots, x^3_{1,k^\star}(t-M+1)],\end{aligned} \quad (10)$$

$$\begin{aligned}\theta_t = [&\theta_1(0), \theta_1(0), \ldots, \theta_1(M+1),\\ &\theta^2(0,0), \theta_2(0,1), \ldots, \theta_2(M-1, M-1),\\ &\theta_3(0,0,0), \theta_3(0,0,1), \ldots, \theta_3(M-1, M-1, M-1)].\end{aligned} \quad (11)$$

Note that the parameter θ was tune by the Nelder-Mead method [16]. This algorithm was based on the concept of the simplex. It sought the maximum of the *CTR* by surrounding in the simpex.

3 Simulation Model

The method was applied for a simulation model which followed the same process as an *in-vivo* setup. A pulse signal was generated digitally and filtered by the transfer function of the ultrasound transducer; centred at 3 MHz with a fractional bandwidth of 90% at −3 dB. It was then sent simultaneously in a microbubble model. Finally, the backscattered signal was filtered by the transfer function of the same ultrasound probe. To take into account imperfections in our simulation, a white noise $\varepsilon(t)$ was added to $x_{p,k}(t)$. The signal to noise ratio (SNR) was chosen at 50 dB.

Note that this model was firstly used linearly. The driving pressure A_0 was set to 1 kPa. This pressure level ensured a linear behavior of the microbubble. Then the model was used nonlinearly where the driving pressure A_0 was set to 400 kPa.

3.1 Microbubbles

The ultrasound contrast agent simulated had properties of encapsulated microbubbles of SonoVue (Bracco Research SpA, Geneva, Switzerland). A phospholipid monolayer with a shear modulus of 46 MPa [17] imprisons sulfur hexafluoride gas (SF_6) [18]. The microbubbles had the following properties:

- mean diameter: 2.5 μm [18];
- shell thickness: 1 nm [19];
- resonance frequency: 3.1 MHz [20].

To carry out the simulations, the free simulation program Bubblesim by Hoff [21] was used to calculate the oscillation and scattered echo for a specified contrast agent microbubble and excitation pulse. A modified version of the Rayleigh-Plesset model was chosen. The properties of the surrounding medium were those of blood, since the microbubble is assumed to be in the vascular system. In order to simulate the mean behavior of the microbubble cloud, we hypothesized that the response of a cloud of N microbubbles was N times the response of a single microbubble with the mean properties.

3.2 Tissue

The tissue response was simulated by fat globules with a density of 928 kg/m^3 [22]. The computation of their response was based on the Rayleigh backscattering [23] for a small fat ball of 10 μm; this size was chosen to approximate the small size of fat cells. We hypothesized that the response of N particles was N times the response of a single particle.

4 Optimization for a Linear System

In this section, we wanted to prove that the random process could find the optimal command. The system studied was thus simplified for a linear system: without pulse inversion technique and where the cost-function was the output energy E'_b backscattered by the microbubble:

$$x_1^\star(t) = \arg\max_{x_1(t)} \left(E'_b(x_1(t))\right). \tag{12}$$

In this case, as for a matched filter, the solution of the optimal command $x_1^\star(t)$ must be the time-reversed output signal $y_1(-t)$. Note that this property was used in time reversal imaging [24].

Fig. 2a represents the best random excitation $x_{1,k^\star}(t)$ and the respective time-reversed output signal of the linear system, among more two hundred and fifty thousand random excitations $x_{1,k}(t)$. The best random excitation was close to the time-reversed response of the linear system. This results confirmed the validity of our approach.

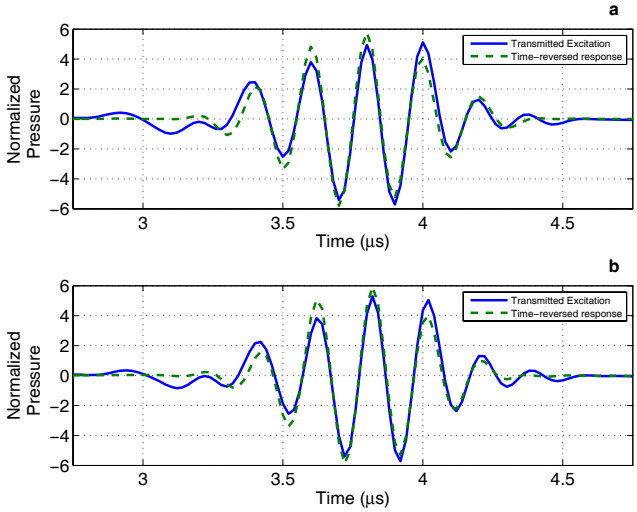

Figure 2: Optimal command for the linear system: (a) obtained by Monte-Carlo method, (b) obtained by Monte-Carlo method and parametric optimization.

Fig. 2b represents the optimal excitation $x_1^\star(t)$ and the respective time-reversed output signal of the linear system after the parametric optimization. The same comments could be done.

However, the table 1 show the backscattered energy and the mean squared error (MSE) between the transmitted excitation and the time-reversed response in each case. After the parametric optimization, the backscattered energy increased and the MSE decreased. The optimal command could be improved by the parametric optimization. Even if the improvement of the parametric optimization was not important, the parametric optimization enabled to be closer to the optimal command. Note that the performances of the parametric optimization depend on the chosen random excitation.

Table 1: Maximum of backscattered energies and the mean squared errors between the transmitted excitation and the time-reversed response in two cases : optimal random excitation (Rand.) and optimal random excitation after random process with parametric optimization (Rand. Opt.)

	Rand.	Rand. Opt.
Backscattered Energy (dB)	77	77.1
Mean Squared Error (dB)	14.7	13.7

Finally, as an illustration, Fig. 3 represents the backscattered energy for each optimization iteration. The optimization converged in eighty iterations.

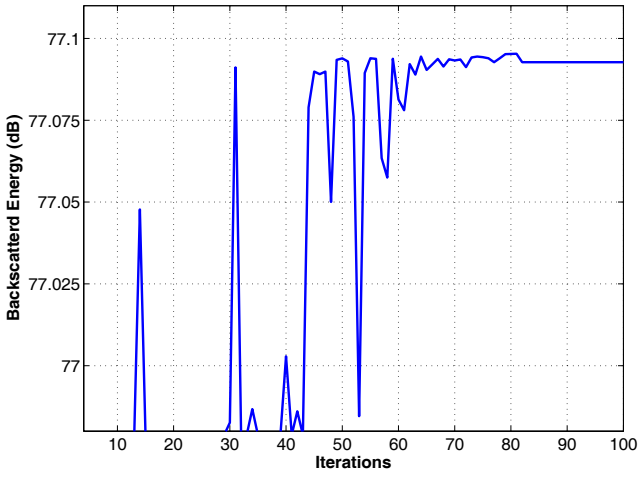

Figure 3: Backscattered energy during the parametric optimization.

To sum up, the optimal command can be find by using random excitations. The research of the optimal command can be improved by adding a parametric optimization. These results confirmed the validity of our approach.

5 Optimization for a Nonlinear Imaging System

In this section, we wanted to find the optimal command to a pulse inversion imaging system in ultrasound contrast imaging. However, when the system behavior was nonlinear, the optimal command was not easy to solve. The command optimal was thus solved by randomness.

Fig. 4a represents the best random excitation $x_{1,k^\star}(t)$ and the respective output signal of the pulse inversion imaging system, among more one million random excitations $x_{1,k}(t)$. The input and the output signals were very different with this nonlinear system. It was difficult to predict this result. Nevertheless note that the best transmitted excitation was amazingly close to the result found by Reddy and Szery [13] in an analytic resolution.

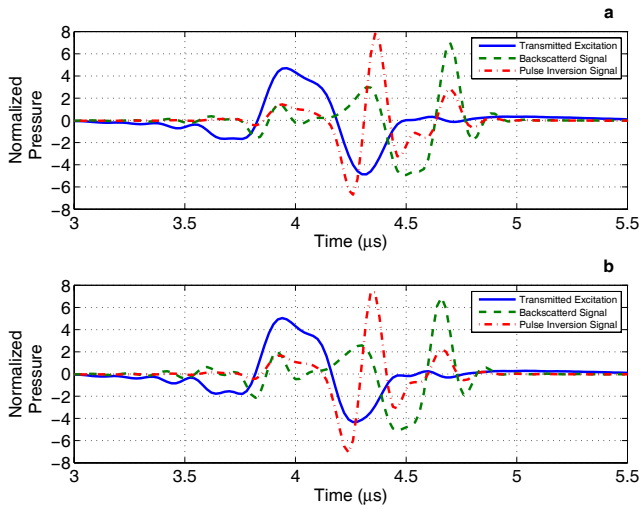

Figure 4: Optimal command for the pulse inversion imaging system: (a) obtained by Monte-Carlo method, (b) obtained by Monte-Carlo method and parametric optimization.

Fig. 4b represents the optimal excitation $x^\star(t)$ and the respective output signal of the pulse inversion imaging system after the parametric optimization. The optimal command was very close to this one obtained randomly.

However, the table 2 shows the *CTR* in four cases : optimal random excitation, optimal random excitation after random process with parametric optimization, sinus wave at the optimal transmit frequency and sinus wave at the centre frequency of the transducer (f_c). It is interesting to note that the excitation usually was a sinus wave modulated by a Gaussian. If the transmit frequency of this sinus wave was the centre frequency of the transducer f_c, the gain between the cases with random excitation and this sinus wave could reach 5 dB and the gain between the cases with random excitation and the optimal sinus wave (*i.e.* $f_{0,opt}$ = 2.5 MHz) could reach 1 dB. Note that the optimization of the transmit frequency was stemed from a previous work [14] extended to the pulse inversion imaging.

Table 2: Maximum of the *CTR* in four cases : optimal random excitation (Rand.), optimal random excitation after random process with parametric optimization (Rand. Opt.), sinus wave at the optimal transmit frequency ($f_{0,opt}$) and sinus wave at the centre frequency of the transducer (f_c).

	Rand.	Rand. Opt.	$f_{0,opt}$	f_c
CTR	31.4 dB	31.5 dB	30.4 dB	26.4 dB

As an illustration, Fig. 5 represents the backscattered energy for each optimization iteration. The optimization converged in eighty iterations.

Finally, the table 3 shows the number of tests to reach different *CTR* with the random process and the random process with parametric optimization. From the command which enabled to obtain *CTR* of 30.54 dB, the random process with optimization enable to decreased around 1, 900 tests to reach a *CTR* of 31.27 dB in comparison with the single random process. The parametric optimization was thus a technique to reach more quickly the optimal command.

To sum up, the optimal command of a nonlinear imaging system can be find by using random excitations. To help the randomness, the parametric optimization can be added to decrease the time of the convergence, when the randomness found a solution close to the optimum.

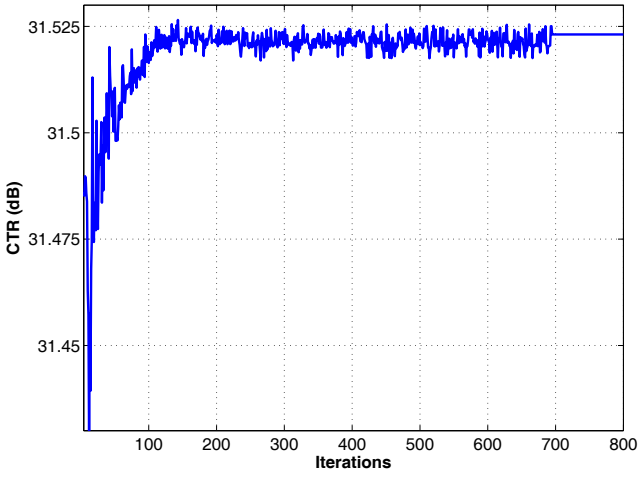

Figure 5: *CTR* during the parametric optimization.

Table 3: Advantage of the parametric optimization for time-consuming property. N_{test} was the minimum number of test to have statistically one excitation which enable to reach *CTR* by the random process (Rand.). For the random process with parametric optimization (Rand. Opt.), the numbers of tests N_{test} was the number of iterations which enabled the *CTR* from the excitation of the example in the first column.

	Rand.		Rand. Opt.
CTR	30.54 dB	31.27 dB	31.27 dB
Probability	$6.6 \cdot 10^{-2}$	$4.6 \cdot 10^{-4}$	-
N_{test}	15	2,165	258

6 Discussions and Conclusion

CTR optimization in pulse inversion imaging was performed randomly, without taking into account *a priori* knowledge of the medium or the transducer. This approach found the optimal command by optimizing the shape directly. Actually, the optimal command enabled the best compromise between the transducer bandwidth and the frequency response of microbubbles and tissue, by maximizing the energy backscattered by microbubbles while minimizing the energy backscattered by the tissue within the transducer bandwidth. To date, this trade-off was usually made empirically for the frequency of sinus waves and it did not enable the best performances.

The ability of our method at finding the optimal command was proved trough a linear system. Consequently, we applied it to a nonlinear imaging system. The implementation method was easy, because the cost-function was exclusively based on the input and the output measurements of our system. Moreover the method was independent of the medium explored. An interesting consequence is that our method can be applied to any imaging system. Nevertheless,

the drawback of our method was the necessary big number of tests to find the optimal command. To help us, we add a parametric optimization to reach the optimal solution more quickly.

Note that the relevant information is currently unknown. Even if the transmit frequency was decisive, it does not explain what differentiates the best random excitations.

To conclude, the method described ensured optimal *CTR* by selecting the optimal command. This work is the first step to automatically find the optimal command. A such solution may improve diagnosis by improving ultrasound image quality.

References

[1] P. J. A. Frinking, A. Bouakaz, J. Kirkhorn, F. J. Ten Cate, and N. de Jong. "Ultrasound Contrast Imaging: Current and New Potential Methods". *Ultrasound Med. Biol.* **26**(6), 965–975 (2000).

[2] M. A. Averkiou. "Tissue Harmonic Imaging". In *Proc. IEEE Ultrason. Symp.* **2**, 1563–1572 (2000).

[3] P. N. Burns. "Instrumentation for Contrast Echocardiography". *Echocardiography* **19**(3),241–258 (2002).

[4] F. Forsberg, W. T. Shi, and B. B. Goldberg. "Subharmonic Imaging of Contrast Agents". *Ultrasonics* **38**(1-8), 93–98 (2000).

[5] A. Bouakaz, S. Frigstad, F. J. Ten Cate, and N. de Jong. "Super Harmonic Imaging, A New Imaging Technique for Improved Contrast Detection". *Ultrasound Med. Biol.* **28**(1), 59–68 (2002).

[6] M.-X. Tang, J.-M. Mari, P. N. T. Wells, and R. J. Eckersley. "Attenuation Correction in Ultrasound Contrast Agent Imaging: Elementary Theory and Preliminary Experimental Evaluation". *Ultrasound Med. Biol.* **34**(12),1998–2008 (2008).

[7] D. H. Simpson, C. T. Chin, and P. N. Burns. "Pulse Inversion Doppler: A New Method for Detecting Nonlinear Echoes from Microbubble Contrast Agents". *IEEE Trans. Ultrason., Ferroelectr., Freq. Control* **46**(2):372–382 (1999).

[8] G. A. Brock-fisher, M. D. Poland, and P. G. Rafter. "Means for Increasing Sensitivity in Non-linear Ultrasound Imaging Systems" *US Patent 5577505* (1996).

[9] P. Phillips and E. Gardner. "Contrast-Agent Detection and Quantification". *Eur. Radiol.* **14**, 4–10 (2004).

[10] J. M. G. Borsboom, A. Bouakaz, and N. de Jong. "Pulse Subtraction Time Delay Imaging Method for Ultrasound Contrast Agent Detection". *IEEE Trans. Ultrason., Ferroelectr., Freq. Control* **56**(6),1151–1158 (2009).

[11] J. M. G. Borsboom, C. T. Chin, A. Bouakaz, M. Versluis, and N. de Jong. "Harmonic Chirp Imaging Method for Ultrasound Contrast Agent". *IEEE Trans. Ultrason., Ferroelectr., Freq. Control* **52**(2), 241–249 (2005).

[12] S. Ménigot. *Commande optimale appliquée aux systèmes d imagerie ultrasonoref*. PhD thesis, Université François-Rabelais de Tours, Tours, France (2011).

[13] A. J. Reddy and A. J. Szeri. "Optimal Pulse-Inversion Imaging for Microsphere Contrast Agents". *Ultrasound Med. Biol.* **28**(4), 483–494 (2002).

[14] S. Ménigot, A. Novell, A. Bouakaz, and J.-M. Girault. "Improvement of the Power Response in Contrast Imaging with Transmit Frequency Optimization". In *Proc. IEEE Ultrason. Symp.*, 1–4 (2009).

[15] P. Phukpattaranont and E. S. Ebbini. "Post-Beamforming Second-Order Volterra Filter for Pulse-Echo Ultrasonic Imaging". *IEEE Trans. Ultrason., Ferroelectr., Freq. Control* **50**(8), 987–1001 (2003).

[16] J. A. Nelder and R. Mead. "A Simplex Method for Function Minimization". *The Computer Journal* **7**(4), 308–313 (1965).

[17] H. J. Vos, F. Guidi, E. Boni, and P. Tortoli. "Method for Microbubble Characterization Using Primary Radiation Force". *IEEE Trans. Ultrason., Ferroelectr., Freq. Control* **54**(7), 1333–1345 (2007).

[18] C. Greis. "Technology Overview: SonoVue (Bracco, Milan)". *Eur. Radiol. Suppl.* **14**(8), 11–15 (2004).

[19] K. Chetty, C. A. Sennoga, J. V. Hainal, R. J. Eckersley, and E. Stride. "P1F-4 High Speed Optical Observations and Simulation Results of Lipid Based Microbubbles at Low Insonation Pressures". In *Proc. IEEE Ultrason. Symp.*, 1354–1357 (2006).

[20] S. M. van der Meer, M. Versluis, D. Lohse, C. T. Chin, A. Bouakaz, and N. de Jong. "The Resonance Frequency of SonoVue(TM) as Observed by High-SpeedOptical Imaging". In *Proc. IEEE Ultrason. Symp.* **1**, 343–345 (2004).

[21] L. Hoff. *Acoustic Characterization of Contrast Agents for Medical Ultrasound Imagingf*, chapter 3, 158–160. Kluwer Academic, Boston, USA (2001).

[22] Thomas Szabo. *Diagnostic Ultrasound Imaging: Inside Outf*. Academic Press, Oxford, UK (2004).

[23] J. W. S. Rayleigh. *The Theory of Soundf* **2**, chapter 15, 149–154. Macmillan (1896).

[24] M. Fink. "Time-reversal of Ultrasonic Fields .1. Basic Principles". *IEEE Trans. Ultrason., Ferroelectr., Freq. Control* **39**(5), 555–566 (1992).